

RESEARCH ARTICLE

Robust multiple method comparison and transformation

Florian Dufey*

Roche Diagnostics GmbH, Germany

Correspondence

*Florian Dufey, Roche Diagnostics GmbH,
Assay Development & System Integration
(CC HetIA) (DSRIBF), Nonnenwald 2,
82377 Penzberg / Germany. Email:
florian.dufey@roche.com

Abstract

A generalization of Passing–Bablok regression for the simultaneous comparison of multiple methods is proposed. Possible applications include assay migration studies or interlaboratory trials. The method is shown to reduce to the usual Passing–Bablok estimator if only two methods are compared. It is close in spirit to reduced major axis regression, which is, however, not robust. To obtain a robust estimator, the major axis is replaced by the (hyper-)spherical median axis. The method is applied to the comparison of SARS-CoV-2 serological tests, bilirubin in neonates, and to a clinical test using different instruments, sample preparations and reagent lots. Plots, similar to the well known Bland–Altman plots, are developed for a posteriori checks of the assumed variance structure.

KEYWORDS:

method comparison, regression, Passing–Bablok regression, clinical statistics, Bland–Altman plots

1 | INTRODUCTION

Method comparison regression is a statistical tool used to compare measurements from a sample set, e.g. blood samples taken from a patient collective, with different methods, like different instrument platforms, assay versions or performed in different laboratories, assuming an underlying linear relation. In contrast to linear regression, none of the methods being compared is assumed to be free of error. Rather, some relation between the methods' standard deviations is assumed. While this kind of problems is prominent in clinical chemistry, the methodology is in no respect restricted to this field. Bablok and Passing¹ proposed a robust estimator for the comparison of two measurements which became known as Passing–Bablok regression (PBR). In contrast to an earlier proposal², this estimator is equivariant under a scaling of the axes and may also be used to perform method transformations, i.e., finding the conversion factor between methods without making the assumption, that this factor is close to 1. The mathematical basis of this method was recently clarified further³. It may be considered a close relative of the more

⁰**Abbreviations:** ARE: asymptotic relative efficiency, EM: Expectation maximization, PBR: Passing–Bablok regression, RMR: reduced major axis regression, mPBR, mRMR: multivariate PBR and RMR, respectively

well known estimator from reduced (or scaled) major axis regression (RMR). The RMR has been extended⁴ for the comparison of more than two methods and is very useful for the analysis of inter-laboratory comparisons or for the calibration of new analytical standards using multiple test formats, however, like RMR, this method is not robust against to outlying measurements. This multivariate extension of the RMR (mRMR) yields compatible estimators in the sense that if $\hat{\beta}_{xy}$ is the slope estimator for the two sets $x = \{x_i\}$ and $y = \{y_i\}$, and $\hat{\beta}_{xz}$ and $\hat{\beta}_{yz}$ the corresponding estimator between x or y and a third set z , respectively, then $\hat{\beta}_{xy}\hat{\beta}_{yz} = \hat{\beta}_{xz}$.

Neither the usual RMR nor PBR with only two variables yield compatible estimates, if slope estimates between more than two variables are compared. Given that measurements in biological samples often show high variability and are prone to outliers, it is desirable to extend the robust PBR to the multivariate case, so that both robust and consistent slope estimates result.

The idea behind the mRMR is to find a scaling of the axes so that the major axis becomes equal to the space diagonal. The major axis is an eigenvector of the estimated covariance matrix, which is not robust. In the following, a multidimensional Passing–Bablok regression (mPBR) is proposed, which reduces to ordinary PBR in two dimensions and yields compatible slope estimates in more than two dimensions. To this end, the (hyper-)spherical median axis⁵ is used instead of the major axis in mRMR with the spherical median axis being a concept from directional statistics⁶. This seems a natural generalization of the usual PBR as it was observed³ that the PBR can be obtained as the slope of a circular median axis in the two-dimensional case.

In the following chapters, a derivation of the new estimator from the spherical median axis will be given. The new method will be applied to the comparison of SARS-CoV-2 serological tests⁷, plasma bilirubin from neonates tests and to the comparison of a clinical test using different sample preparation methods, instrument platforms and reagent lots. In the latter example, the utility of the new method to analyze differences between sub-groups is demonstrated.

2 | DERIVATION OF THE HYPER-SPHERICAL MEDIAN AXIS ESTIMATOR

2.1 | General situation

Consider a sample of size n where elements are labeled by $i \in \{1, \dots, n\}$ and each element is measured with N different methods to be arranged into an array with components $x_{i\mu}$ with $\mu \in \{1, \dots, N\}$. The values $x_{i\mu}$ are assumed to follow the model

$$x_{i\mu} = \beta_{\mu}r_i + \epsilon_{i\mu} + \alpha_{\mu},$$

where $\beta = \{\beta_{\mu}\}$ is the slope vector, the scalar r_i is proportional to the unknown true concentration of sample i , $\alpha = \{\alpha_{\mu}\}$ is the intercept vector and $\epsilon_i = \{\epsilon_{i\mu}\}$ is the vector of random errors. The random errors are assumed independent for $i \neq j$, while the distributions of $\epsilon_{i\mu}$ and $\epsilon_{i\nu}$ are similar and independent, so that the variance matrix $\Sigma_i = \Gamma\sigma_i^2$ is diagonal and the variance ratios for different instruments is independent of i . In the derivation of the mPBR this form will be specialized to $\Gamma_{\mu\mu} = \beta_{\mu}^2$.

Otherwise the error distributions may be quite arbitrary, especially, normality is not assumed and, due to the σ_i which may differ from sample element to element, the errors may be heteroscedastic. This generalizes the assumptions made in Bablok et al.¹ for the comparison of two methods. The distribution of the instrumental variables r and errors ϵ can be discussed in either a structural, functional or ultrastructural model setting. An even more useful equivalent expression is

$$y_{i\mu} := b_\mu x_{i\mu} = r_i + \tilde{\epsilon}_{i\mu} + a_\mu,$$

with the vector of inverse slopes $b := \{1/\beta_\mu\}$, which may be interpreted as scaling factors, the scaled intercept parameters $a_\mu = b_\mu \alpha_\mu$ and $\tilde{\epsilon}_{i\mu} = b_\mu \epsilon_{i\mu}$. It is clear that the b_μ , r_i and a_μ can only be estimated up to a common overall factor, which fixes the scale of the concentrations r_i .

The scaled values $y_{i\mu} := b_\mu x_{i\mu}$ are then symmetrically distributed in space around the axis $y(\lambda) = \lambda e + a$ along the space diagonal e with $e_\mu = 1/\sqrt{N}$ for all μ .

First, the situation $a = 0$ is considered: I.e., the expected regression line will pass through the origin. In the mRPR, the estimated slope/scaling vector $\hat{\beta}$ is obtained from uncentered principal component analysis: The equations for the ordinary, i.e. not reduced, major axis regression, also known as Deming-regression, are obtained by minimization of the sum of squares

$$L = \sum_i (x_i - \beta r_i)^T \Sigma_i^{-1} (x_i - \beta r_i). \quad (1)$$

with respect to the r_i and β . This yields the estimates

$$\hat{r}_i = \frac{\hat{\beta}^T \Gamma^{-1} x_i}{\hat{\beta}^T \Gamma^{-1} \hat{\beta}}$$

and subsequently an equation for $\hat{\beta}$,

$$\sum_i \sigma_i^{-2} (\hat{\beta}^T \Gamma^{-1} x_i) \left(I_n - \frac{\Gamma^{-1/2} \hat{\beta} \hat{\beta}^T \Gamma^{-1/2}}{\hat{\beta}^T \Gamma^{-1} \hat{\beta}} \right) \Gamma^{-1/2} x_i = 0, \quad (2)$$

where I_N is the $N \times N$ diagonal unit matrix.

Obviously, this are just the well known equation of weighted major axis regression. However, measurements with a large value of r will have a high leverage whence the method is not robust against outliers. This is also true for mRPR: The equation for the slope $\hat{\beta}$ follows upon setting $\Gamma_{\mu\mu} = \hat{\beta}_\mu^2$ in Eq. 2,

$$\sum_i \sigma_i^{-2} (e^T y_i) (I_N - e e^T) y_i = 0. \quad (3)$$

The alternative mPBR algorithm uses ideas from finding the spherical median axis⁵, cf. Fig. 1. In the spirit of most robust regression methods, the weighting with σ_i^{-2} is disregarded. It is clear that the matrix Γ^{-1} induces a metric which by scaling the original β and x_i can be made a unit metric.

Rays passing through the origin and the scaled points $\Gamma^{-1/2}x_i$ are considered. These will intersect the unit sphere at two antipodal points $\widetilde{\Gamma^{-1/2}x_i} = \pm\Gamma^{-1/2}x_i/|\Gamma^{-1/2}x_i|$, where the hajecc accent signifies normalization of the vector to unit length. The circular median axis is now the line defined by the unit vector \check{s} with smallest sum of distances to all points $\widetilde{\Gamma^{-1/2}x_i}$ on the same hemisphere, i.e.,

$$\arg \min_{\check{s}} \sum_i \arccos \left(\left| \check{s}^T \widetilde{\Gamma^{-1/2}x_i} \right| \right). \quad (4)$$

For Γ being a unit matrix, the situation is illustrated in Fig. 1. We might call this figuratively the sky-mongers regression, thinking of the points $\widetilde{\Gamma^{-1/2}x_i}$ as positions of the stars of some constellation on the celestial sphere and the point \check{s} on the sphere as the center of the respective constellation, fixing the line of sight of the sky-monger to \check{s} .

As long as none of the $\widetilde{\Gamma^{-1/2}x_i}$ falls directly on the axis defined by \check{s} , the dependence on \check{s} is analytical whence the minimum is attained if

$$\sum_i \operatorname{sgn}(\check{s}^T \Gamma^{-1/2}x_i) \frac{(I_N - \check{s}\check{s}^T)\Gamma^{-1/2}x_i}{|(I_N - \check{s}\check{s}^T)\Gamma^{-1/2}x_i|} = 0. \quad (5)$$

This regression, while being a robust alternative to Deming regression does not yield unbiased estimates of the slopes for general error distributions, maybe with the exception of normally distributed errors.

More attractive is the equivalent of the mRPR, the mPBR, obtained by setting $\Gamma_{\mu\mu} = \hat{\beta}_\mu^2$ in Eq. 5. The situation is modified insofar¹ as the median \check{s} of the scaled y_i is known to coincide with the space diagonal e , so that Eq. 5 now becomes an equation for the estimated scaling vector \hat{b} .

$$\arg \min_{\check{s}} \sum_i \arccos \left(\left| \check{s}^T X_i \hat{b} \right| \right) = e. \quad (6)$$

In the derivation of this equation, it was used that $\Gamma^{-1/2}x_i = X_i \hat{b}$ with the diagonal matrix X_i with $X_{i,\mu\mu} = x_{i,\mu}$.

Hence,

$$\sum_i \operatorname{sgn}(x_i^T \hat{b}) \frac{P X_i \hat{b}}{|P X_i \hat{b}|} = 0, \quad (7)$$

where $P = (I_N - ee^T)$ is the projection matrix to the hyperplane perpendicular to e . Comparing Eqs. 3 and 7, the latter differs from the former by the missing weighting with σ_i , the replacement of $e^T y_i$ by its sign, and the replacement of $P y_i$ by a unit vector pointing in the same direction. Clearly the effect of each term is bounded by ± 1 , so that the estimate becomes robust.

The actual slope estimator of measurement ν vs μ is $\hat{\beta}_{\mu\nu} = \hat{b}_\mu / \hat{b}_\nu$.

These estimators fulfill the consistency condition $\hat{\beta}_{\mu\nu} \hat{\beta}_{\nu\kappa} = \hat{\beta}_{\mu\kappa}$. It should be clear that, without further information, r and b can only be estimated up to a common scaling factor. This factor may be fixed as convenient, e.g. the choice $\hat{b}_1 = 1$ would set the scale to that of the first method. Then, the $\hat{\beta}_\mu = 1/\hat{b}_\mu$ with $\mu > 1$ are the $N - 1$ slopes relative to that of the first method $\hat{\beta}_1 = 1$.

¹Curiously, a scaling of the celestial sphere in the star-monger scenario can be physically implemented in Einstein's special relativity by boosting to another inertial system⁸

If the intercept parameters are a priori not known to be 0, in the spirit of Theil–Sen and Passing–Bablok regression, the estimation of the scaling parameters b can be decoupled from the estimation of the intercept parameters a replacing the x_i in Eq. 7 with the differences $\Delta x_J := x_j - x_i$ with $i < j$ and extension of the sum to the corresponding index pairs $\{J\} := \{(i, j)\}$,

$$\sum_J \operatorname{sgn}(\Delta x_J^T \hat{b}) \frac{P \Delta x_J \hat{b}}{|P \Delta x_J \hat{b}|} = 0. \quad (8)$$

In two dimensions, writing $x_i = (x'_i, y'_i)^T$ and $\hat{b} = (1, \hat{m})^T$, Eq. 8 may be simplified to

$$\sum_J \operatorname{sgn}(\Delta y'_J + \hat{m} \Delta x'_J) \operatorname{sgn}(\Delta y'_J - \hat{m} \Delta x'_J) = 0.$$

which coincides with the defining equation of the pairwise PBR³.

To render the definition of the intercept vector unique it is convenient to chose $e^T a = 0$, so that

$$E \left(\frac{x_i^T b}{N} \right) = r_i$$

which leads to using

$$\hat{r}_i = \frac{x_i^T \hat{b}}{N}$$

as an estimator for r_i . A robust estimator for the intercept vector \hat{a}_μ can then be obtained from the spatial median SpMed^9 ,

$$\hat{a}_\mu := \operatorname{SpMed}(\{P x_i \hat{b}\}).$$

The spatial median SpMed is defined as the point with minimal distance

$$\operatorname{SpMed}(\{x_i\}) = \arg \min_y \sum_i d(x_i - y),$$

where $d(x)$ is the usual Euclidean norm of the vector x . This is equivalent to

$$\sum_i \frac{x_i - \hat{y}}{|x_i - \hat{y}|} = 0$$

as long as \hat{y} does not equal any of the x_i (adaptions for this situation are easily devised).

From the intercept parameter vector \hat{a} the intercept $\alpha_{\mu\nu}$ for the graph of x_ν vs. x_μ , $\hat{\alpha}_{\mu\nu}$, can be calculated as

$$\hat{\alpha}_{\mu\nu} = \frac{\hat{a}_\nu - \hat{a}_\mu}{\hat{b}_\nu} = \hat{\alpha}_\nu - \hat{\alpha}_\mu \frac{\hat{b}_\mu}{\hat{b}_\nu}.$$

3 | NUMERICAL IMPLEMENTATION AND IMPUTATION OF MISSING MEASUREMENTS

There are at least two reasons why it seems important to impute missing measurements:

Firstly, with increasing dimension N , the probability of randomly missing elements increases and it becomes less and less economical not being able to use the other measurements of the vector x_i .

Secondly, it is possible that only a subset of all components can be measured at a certain time. As an example, we consider that at a certain point of time 3 reagent lots are being compared with a panel of patient samples. At a later time, the measurement is repeated using a new sample panel. While, say, reagent lots 2 and 3 are still available, reagent lot 1 is no longer available and instead a new reagent lot number 4 is included in the comparison. Analysis of the combined set of measurements is highly desirable as it allows estimation of consistent slope parameters b_μ for all for reagent lots, although none of the patient samples has been measured with all lots. With imputation it becomes possible to get estimates for all 4 lots. If such a series of measurements is extended to a longer time span, it becomes possible to track changes of the parameters a and b with time.

A solution of equation 8 (and analogously Eq. 7) can be found by iterative reweighting^{9,10}. To solve Eq. 8, approximate values for the weights

$$w_J^{(n)} = \frac{\text{sgn}(\Delta x_J^T \hat{b}^{(n)})}{|P \Delta x_J \hat{b}^{(n)}|}$$

may be calculated with the current estimator of the slopes $\hat{b}^{(n)}$ (a starting value could be all $\hat{b}_\mu^{(0)} = 1$), and then an improved estimator $\hat{b}_\mu^{(n+1)}$ may be derived as a solution of the linear equation system

$$\sum_J w_J^{(n)} P \Delta x_J \hat{b}^{(n+1)} = 0.$$

Analogously, the spatial median estimate of the intercept \hat{a} may be computed, either after a converged estimate of the slope has been obtained from

$$\sum_i v_i^{(n)} P(\hat{a}^{(n+1)} - x_i \hat{b}) = 0$$

with weights $v_i^{(n)} = |P(\hat{a}^{(n)} - x_i \hat{b})|$, or simultaneously, replacing \hat{b} with $\hat{b}^{(n+1)}$ in these equations. The simultaneous procedure offers the advantage that it becomes possible to impute missing observations in the spirit of an expectation-maximization (EM) algorithm¹¹. Namely, if the component $x_{i\mu}$ is missing, an estimate of the missing value is

$$\hat{x}_{i\mu}^{(n)} = (\hat{a}_\mu^{(n)} + \hat{r}_i^{(n)}) / \hat{b}_\mu^{(n)}$$

with

$$\hat{r}_i^{(n)} = \frac{\sum_{v \notin \{\mu_i\}} (x_{iv} \hat{b}_v^{(n)} - a_v^{(n)})}{N - \#\{\mu_i\}}.$$

Here, $\{\mu_i\}$ are the indices μ of the missing elements of x_i . Slight extensions of the Weiszfeld¹⁰ algorithm for the spatial median, can be proven to converge always. Eventually it is possible to implement similar extensions for the slope estimation.

4 | STATISTICAL PROPERTIES OF THE MULTIVARIATE PBR ESTIMATOR

The examples shown in the next section demonstrate the potential of the new method, however, a formal proof of its statistical properties is not in scope of this article. Nevertheless it seems appropriate to at least discuss some concepts and compare to related estimators. Detailed proofs will also depend on the assumed model setting, e.g. structural, functional or ultrastructural¹².

Consistency For most models settings, it is to be assumed that the mPBR estimator is consistent due to the symmetry of the model with respect to exchange of the measurements.

Finite sample bias It is known³ that the estimates for the components of b are biased in case of RMR and also ordinary PBR, while the logarithms $\ln \hat{b}$ are unbiased. It seems plausible that this also the case for the estimators \hat{b} from mPBR in more than two dimensions.

Asymptotic efficiency An asymptotic relative efficiency (ARE) of $\pi/4$ was reported⁵ for the spherical median axis assuming the distribution of the points on the sphere to follow a Watson distribution in the limit of small dispersion parameter. This coincides with the ARE of the spatial and spherical median. Because the mPBR, in contrast to the (spherical) median, is not an M-, but only a Z-type estimator, these results cannot be directly adopted. Comparing the variances of the PBR to that of the RMR in two dimensions and assuming a Gaussian distribution, a relative asymptotic efficiency of $9/\pi^2$ was reported³.

Robustness As the angle on the sphere is bounded, the mPBR slope estimator is robust against outlying points. As the possible angles between the space diagonal and a line through 2 points does not depend on the dimension of the space, the breakdown point will be independent of dimension. For the two-dimensional case, the breakdown point is $1 - \sqrt{2}/2$, as for Theil–Sen regression³.

Numerical complexity The proposed algorithm is not optimal with respect to its numerical complexity, as it scales quadratically with the number of measurements n . In the two-dimensional case, a reduction to a quasilinear scaling with n is possible¹³. Whether similar algorithms can be devised in the multidimensional case, is an interesting question.

Uncertainty The very concept of confidence limits for the slope in method comparison is highly problematic due to the Gleason phenomenon¹². Expressions were derived³ for the asymptotic variance of the slope and intercept of the PBR. Also bootstrapping seems to be a valuable alternative¹³.

Identifiability Method comparison and, in more generality, errors in variable models, suffer from the problem that the individual variances of the methods being compared cannot in all cases be estimated from the data used in regression¹⁴. Even in situations, where an estimation is theoretically possible, the corresponding estimators are based on moments of higher

order, which in practice can mostly not be estimated with sufficient precision. Therefore, most methods used for method comparison make assumptions about the error structure and variance ratios and mPBR is no exception. Hence one should keep in mind that the smaller the correlation of the data, the larger the possible error due to misspecification of the variance ratio.

5 | EXAMPLES

5.1 | Multidimensional regression of SARS-CoV-2 measurement data

The methodology developed above was applied to find a regression line through data (cf. Ferrari et al.⁷) from 48 samples measured with 6 different quantitative SARS-CoV-2 serological tests² (Fig. 3) and the estimates for the slopes obtained with the mPBR was compared to the pairwise Passing–Bablok estimates. The correlation between the different tests is generally quite poor. Kendall’s correlation coefficient τ ranges from 0.5 between the DiasTrim and the Euroimmun test and 0.79 between the Roche and the DS test. Slope estimators obtained with the multivariate method are mostly less extreme, i.e. closer to 1 than the Passing–Bablok estimators. While the mPBR estimators are consistent by design, there are considerable inconsistencies between the pairwise Passing–Bablok estimators. For example, the estimators of DS vs. DiasTrim and Euroimmun are 3.73 and 3.28, respectively, from which an DiasTrim vs. Euroimmun estimator of $3.28/3.73 = 0.88$ can be calculated, which is more than 60% larger than the one from direct comparison, 0.54. In Fig. 4 the estimated intercept parameters are plotted versus the inverse slope parameters, yielding a more condensed representation of the regression estimates. The large differences in slope between some of the assays are due to the use of assay specific standards (U/mL), different from the international standard established by the WHO who defined binding antibody units per milliliter (BAU/mL). Therefore, this analysis is rather of the method transformation than the method comparison type and may be used to calculate conversion factors. For the Roche, Euroimmun and DS test, a conversion factor of 1 BAU/U is reported by the manufacturers. For the Siemens and Diastrim assay conversion factors of 21.8 BAU/U and 2.6 BAU/U were reported by the manufacturers. No conversion factor was reported for the DiaS1S2 test. As far as the relatively small intercepts can be neglected, a conversion factor may be estimated for this last test: Dividing the \hat{b}_μ values by the manufacturer supplied conversion factors for the 5 tests, for which the factor was available, and taking the geometric mean, yields a mean value $\bar{b} = 0.404$ on the WHO BAU/mL scale. Division of the DiaS1S2 inverse slope parameter $\hat{b} = 1.63$ by this mean yields a conversion factor of 4.04 BAU/U for this test.

Finally, in Fig. 5, the deviation (“Standardized residuals”) of the y_i from the mean $\hat{f}_i + \hat{a}$, on a common scale, are plotted as a function of \hat{f}_i (“Mean”), which is close in spirit to Bland–Altman plots¹⁵. The standard deviations seem to increase linearly

²Full names of the tests and abbreviations used in the text and captions: Diasorin LIAISON SARS-CoV-2 Trimerics IgG (DiasTrim), Euroimmun Anti-SARS-CoV-2 (Euroimmun), Roche Elecsys®Anti-SARS-CoV-2-S (Roche), DIESSE CHORUS SARS-CoV-2 “NEUTRALIZING” Ab (DS), Atellica IM SARS-CoV-2 IgG (Siemens), Diasorin LIAISON SARS-CoV-2 S1/S2 IgG (DiaS1S2)

with r . For mean values below 10000, the errors seem to be highest for the Diastrim, DS and Euroimmun tests, with the DS and Siemens test showing some systematic bias. At higher values ($r > 10000$), the Siemens and DS test show little bias, while the Diastrim and Euroimmun test seem biased to lower and the Roche and DiasS1S2 test to higher values.

5.2 | Bilirubin in neonates

Warner et al.¹⁶ compare total bilirubin measurements in plasma samples from neonates using assays and analysis platforms from different manufacturers³. This article should also be consulted for further details on the assays and the data used below. While the precision within each method was high, the slopes of the PBR line differed considerably from 1 for some methods, which may put neonates with high bilirubin plasma levels at risk not to obtain adequate therapy. The data were re-analyzed using mPBR. In total, 11 samples were measured, most of them in duplicate, but as the second measurement was not available for all systems, only the first measurement was used in the calculations shown below. The pairwise regression line parameters almost coincide with the ones obtained using pairwise PBR, only in the comparisons to one system (VITROS 5600) some slight differences are visible to the eye, see Fig. 6.

The latter system also shows a larger imprecision as compared to the other systems, cf. Fig. 7, confirming the results in¹⁶. As in the previous example, the mPBR allows for a condensed representation of the results from the analysis, see Fig. 8, showing a considerable difference in inverse slope parameters with the Architect ci 16200 on the lower end and the cobas c702 on the other.

5.3 | Comparison of an assay from clinical chemistry

As a third example, the results of a multidimensional method comparison of two different sample preparation methods (A and B), two different measurement platforms (X and Y), and 6 different reagent lots (1 to 6) are shown for a quantitative clinical test using 150 whole blood samples. A Bland–Altman type plot of the residuals versus mean shows no relevant differences between the assays and is therefore not shown.

However, differences between the two sample preparation methods and, to a smaller extent, also between the instrument platforms are clearly visible in the plot of the intercept vs. inverse slope parameters in Fig. 9. These differences may be quantified further using a linear regression of the inverse slope parameters and the intercept parameters on the relevant effects: If x_{pre} is the dichotomic variable of pre-analytical treatment with levels 0 for reference A and 1 for B, and x_{inst} the dichotomic variable of instrument platform with levels 0 for reference X and 1 for Y, the linear model

$$-\ln(b) \sim q_{\text{pre}}x_{\text{pre}} + q_{\text{inst}}x_{\text{inst}}$$

³Names of the analysis platforms and manufacturers: Alinity c and Architect ci16200 (Abbott Diagnostics, USA), AU5822 (Beckman Coulter, USA), cobas@c702 and cobas c502 (Roche Diagnostics, Germany), ABL90 FLEX (Radiometer Denmark)

is fit. The intercept has no relevance, but $\hat{\beta}_{\text{pre}} = \exp(\hat{q}_{\text{pre}})$ and $\hat{\beta}_{\text{inst}} = \exp(\hat{q}_{\text{inst}})$ may be interpreted as the average slope between tests with pre-analytical treatment B vs. A and instrument platform Y vs. X, respectively. For the example, $\hat{\beta}_{\text{pre}} = 0.965$ and $\hat{\beta}_{\text{inst}} = 0.978$ indicate both a difference in slopes due to pre-analytical treatment and a smaller one due to the platform.

Similarly, the intercept parameters a (without taking logarithms) may be fit, yielding $\Delta\hat{a}_{\text{pre}} = 5.55$ and $\Delta\hat{a}_{\text{inst}} = 3.53$.

6 | DISCUSSION

While the comparison of multiple methods is a recurrent standard task in clinical chemistry, the methodology usually applied to analyze the results of these comparisons reduces to repeated pairwise comparisons. This is clearly inefficient and reports resulting from these analyses get more convoluted the more methods are being compared. With mRMR, a bespoke methodology was proposed⁴, but this method did not find much use, perhaps because not even pairwise RMR is widespread in clinical chemistry. Therefore, it was the aim of the present article to extend the well established pairwise PBR methodology to the multidimensional setting. Compared to the mRMR, the mPBR technique is robust against outlying measurements, but otherwise comprises the advantages of mRMR, namely in that the slope estimators between pairwise method comparisons are consistent. The estimators are by construction equivariant under a scaling of the individual measurements, which makes the approach applicable not only to method comparison, but also to method transformation. As an example, mPBR was applied to the comparison of SARS-CoV-2 serological tests⁷ some of which were standardized against different standards which results in pairwise slopes vastly different from 1.

If N methods are being compared, only $N - 1$ parameters have to be estimated which allow for the calculation of all $N(N - 1)/2$ pairwise slopes, and likewise $N - 1$ parameters to calculate all intercepts. As shown in the example section, this allows for a much more economical representation of the parameters (cf. Figs. 4, 8, 9) and the variance structure (Figs. 5, 7), than is possible with pairwise tabulations and Bland–Altman plots. More importantly, the inverse slope and intercept parameters, b and a , respectively, allow for further analyses, e.g. of factors determining their value. As an example, in section 5.3 the influence of pre-analytical treatment and instrument platform on the parameters obtained for assays from clinical chemistry was analyzed using linear regression.

As far as the mathematical formulation of the mPBR estimator is concerned (cf. Sect. 4), it is interesting that it relates to the field of directional statistics^{6,5}. Many questions are worthy of further elaboration. For most of the formal statistical properties of the mPBR slope estimator, like its consistence, efficiency or finite sample bias, only educated guesses could be formulated here. Stronger results would make it necessary to specialise to either a structural, functional or ultrastructural model setting¹². Generally, it can be stated that the theoretical basis of method comparison is by far not as developed as that of ordinary, even

nonlinear, regression and brings with it subtle new problems, like the Gleason phenomenon, which basically states that no true confidence intervals can be formulated.

Concerning the practical implementation of the proposed algorithm Eq. 3, at the moment, only a basic variant of the Weiszfeld-algorithm was implemented, which scales at least quadratically with the number of observations and requires all samples to have been measured with all methods. Specifically, the proposed EM-algorithm has not yet been implemented. Both the implementation of an EM based imputation of missing values, and the search for an algorithm with reduced numerical complexity, would be very valuable.

7 | ACKNOWLEDGMENTS

I thank Daniele Ferrari for kindly providing the data for the SARS-CoV-2 example and explaining the background of the study and Jonas Mir for carefully reading the manuscript and very helpful discussions.

ELECSYS and COBAS are trademarks of Roche. All other product names and trademarks are the property of their respective owners.

References

1. Bablok W, Passing H, Bender R, Schneider B. A general regression procedure for method transformation. Application of linear regression procedures for method comparison studies in clinical chemistry, Part III. *J Clin Chem Clin Biochem* 1988; 26: 783–790.
2. Passing H, Bablok W. A new biometrical procedure for testing the equality of measurements from two different analytical methods. Application of linear regression procedures for method comparison studies in clinical chemistry, Part I. *J Clin Chem Clin Biochem* 1983; 21: 709–720.
3. Dufey F. Derivation of Passing–Bablok regression from Kendall's tau. *Int J Biostat* 2020; 16(2).
4. Feldmann U, Schneider B, Klinkers H, Haeckel R. A Multivariate Approach for the Biometric Comparison of Analytical Methods in Clinical Chemistry. *J Clin Chem Clin Biochem* 1981; 19(3): 121–138. doi: doi:10.1515/cclm.1981.19.3.121
5. Fisher N, Lunn A, Davies S. Spherical median axes. *J R Stat Soc Ser B (Method)* 1993; 55(1): 117–124.
6. Mardia KV, Jupp PE, Mardia K. *Directional statistics*. 2. Wiley Online Library . 2000.
7. Ferrari D, Clementi N, Spanò SM, et al. Harmonization of six quantitative SARS-CoV-2 serological assays using sera of vaccinated subjects. *Clin Chim Acta* 2021; 522: 144–151. doi: <https://doi.org/10.1016/j.cca.2021.08.024>

8. Oblak B. From the Lorentz group to the celestial sphere. *arXiv preprint arXiv:1508.00920* 2015.
9. Weiszfeld E. Sur le point pour lequel la somme des distances de n points donnés est minimum. *Tohoku Math J* 1937; 43: 355–386.
10. Beck A, Sabach S. Weiszfeld’s method: Old and new results. *J Optim Theory Appl* 2015; 164(1): 1–40.
11. Dempster AP, Laird NM, Rubin DB. Maximum likelihood from incomplete data via the EM algorithm. *J R Stat Soc: Ser B (Method)* 1977; 39(1): 1–22.
12. Cheng CL, Van Ness JW. *Statistical regression with measurement error*. Arnold . 1999.
13. Raymaekers J, Dufey F. Equivariant Passing–Bablok regression in quasilinear time. *arXiv preprint arXiv:2202.08060* 2022.
14. Reiersøl O. Identifiability of a linear relation between variables which are subject to error. *Econometrica* 1950; 18: 375–389.
15. Bland JM, Altman D. Statistical methods for assessing agreement between two methods of clinical measurement. *Lancet* 1986; 327(8476): 307–310.
16. Thomas DH, Warner JV, Jones GR, et al. Total bilirubin assay differences may cause inconsistent treatment decisions in neonatal hyperbilirubinaemia. *Clin Chem Lab Med* 2022; 60(11): 1736–1744.



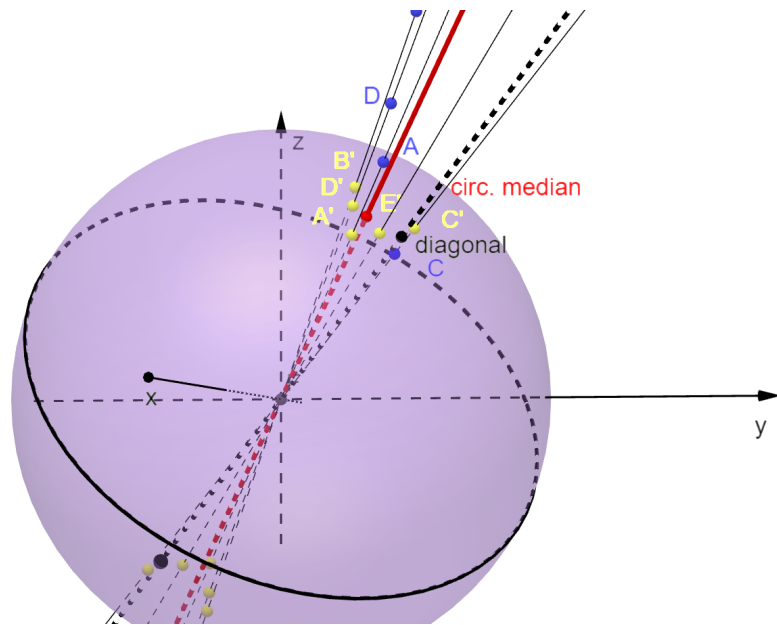


Figure 1 Spherical median axis (red) of 5 points (A–E, blue). The yellow points A'–E' are the projections of the points on the sphere. The red point corresponding to s designates the position of the spherical median. It has the smallest angular distance on the sphere to the points A'–E'. Only the points on the same hemisphere as s are taken into account. A unit metric with $\Gamma_{\mu\mu} = 1$ was assumed for illustration.

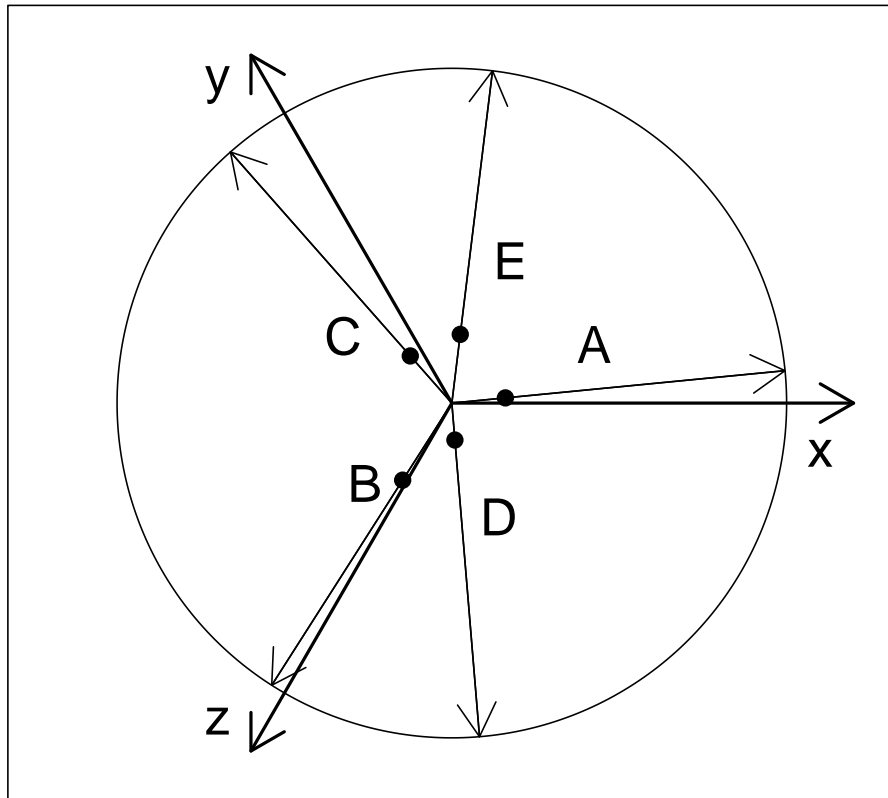


Figure 2 Visualisation of the mPBR algorithm with zero intercepts: The points are scaled with the \hat{b}_μ until the unit vectors passing through the points $A - D$ (filled dots) in the plane perpendicular to the space diagonal sum up to 0.

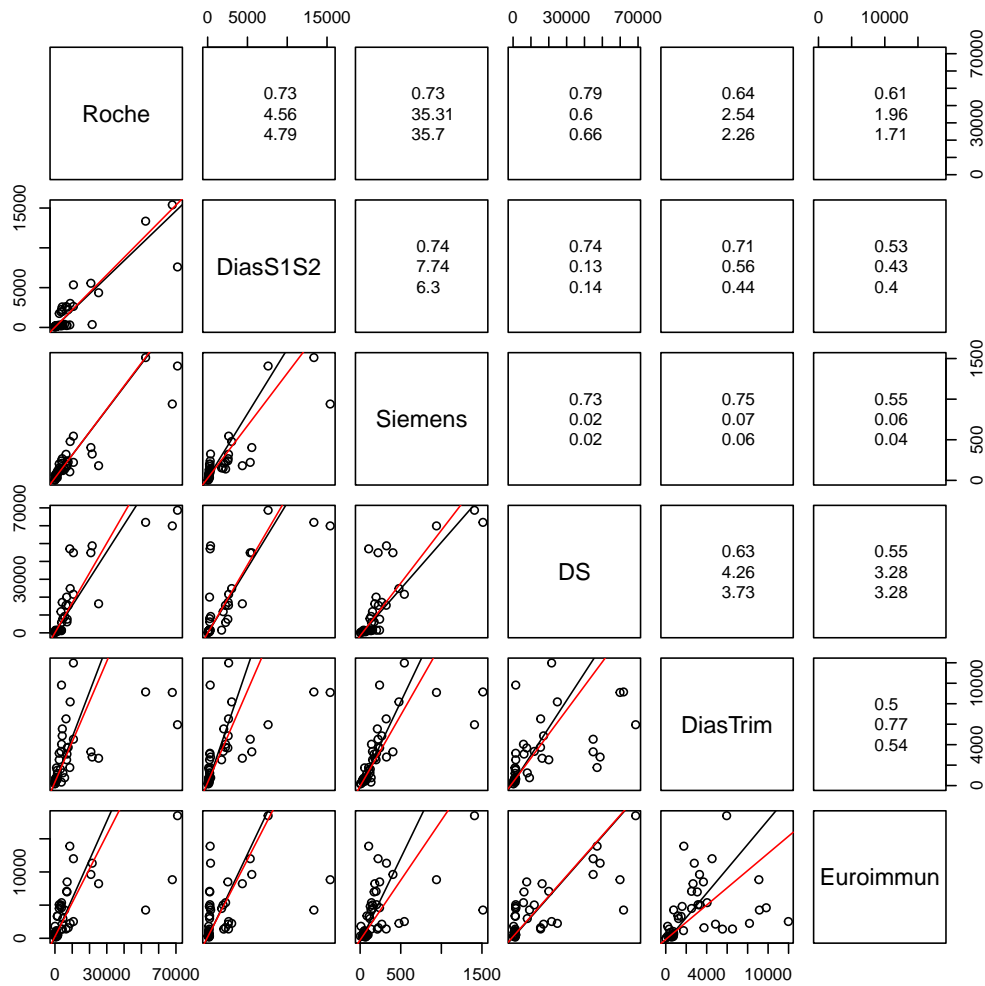


Figure 3 Comparison of mPBR (red lines) to pairwise PBR (black lines) in the SARS-CoV-2 test example. In the upper triangle, Kendall's correlation coefficient τ , slope estimates obtained with mPBR (center) and pairwise PBR (bottom) are reported. The unit on all axes is U/mL.

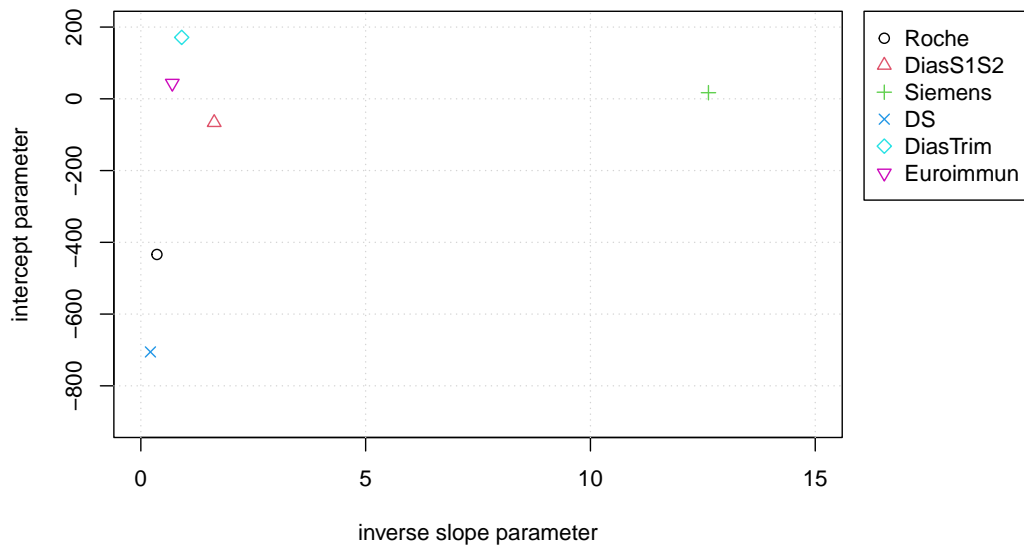


Figure 4 Intercept vs. inverse slope parameters of the various SARS-CoV-2 serological tests (referring to U/mL). Large differences, especially in b , can be explained by units U being manufacturer specific.

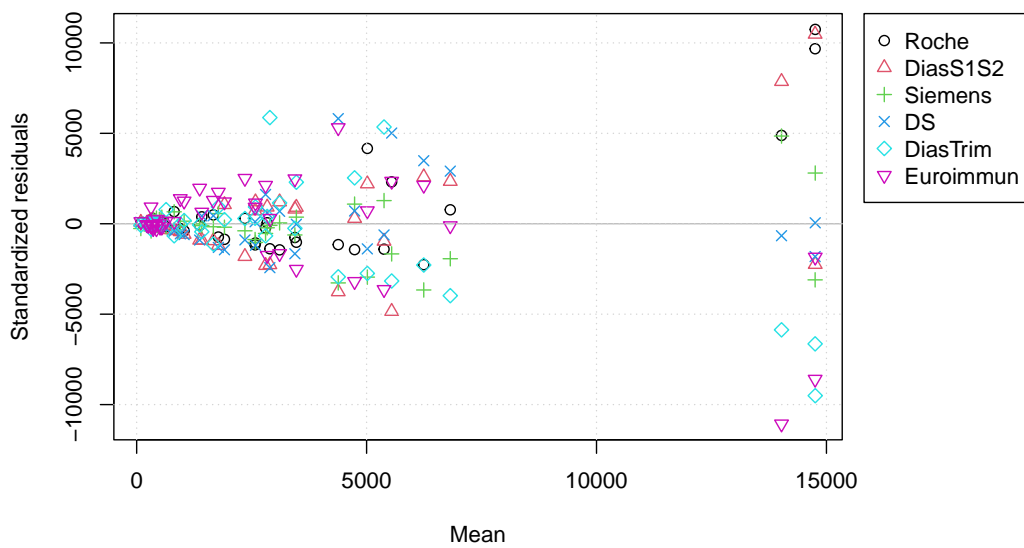


Figure 5 Generalized Bland–Altman plot for the SARS-CoV-2 serological tests with $y_i - r_i - a_i$ (Standardized residuals) on the ordinate and r_i values (Mean) on the abscissa.

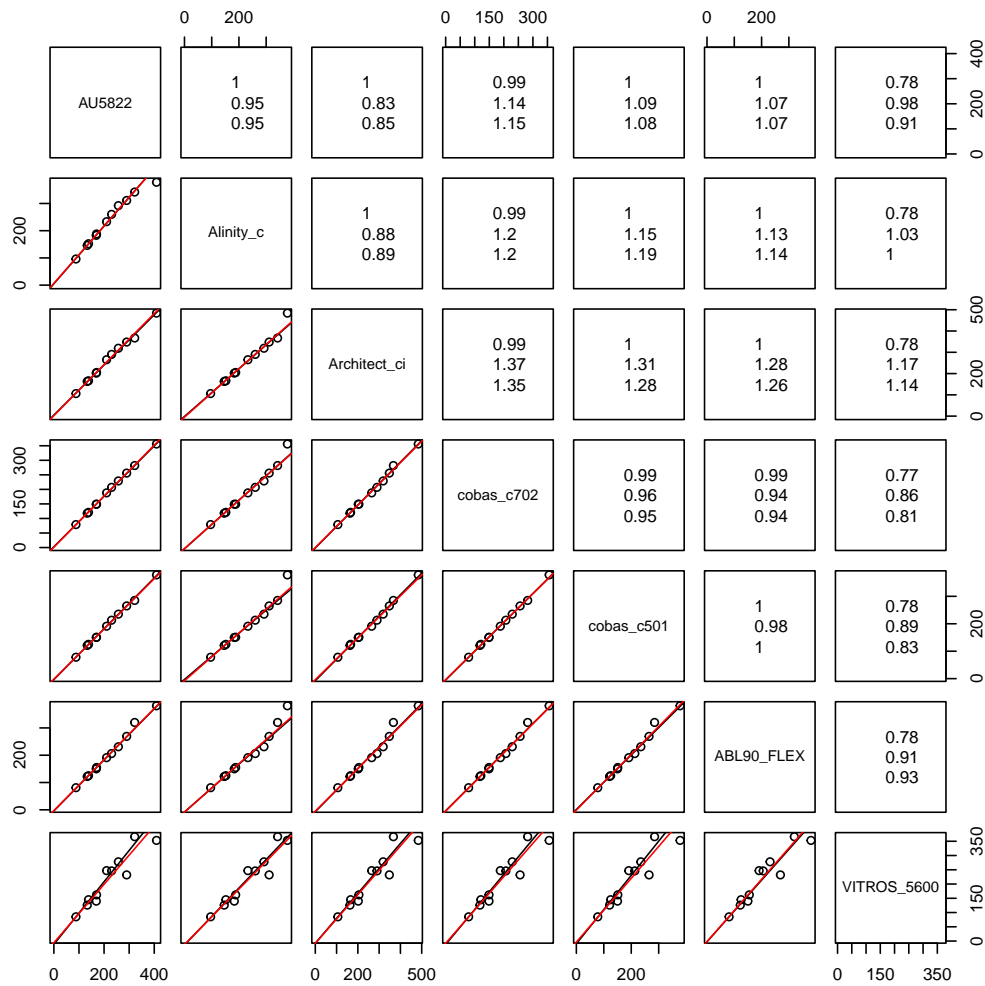


Figure 6 Comparison of 11 neonate total bilirubin plasma samples (concentration in $\mu\text{mol/L}$) with 7 different assays with mPBR (red lines) and pairwise PBR (black lines). In the upper triangle, Kendall's correlation coefficient τ , slope estimates obtained with mPBR (center) and pairwise PBR (bottom) are reported.

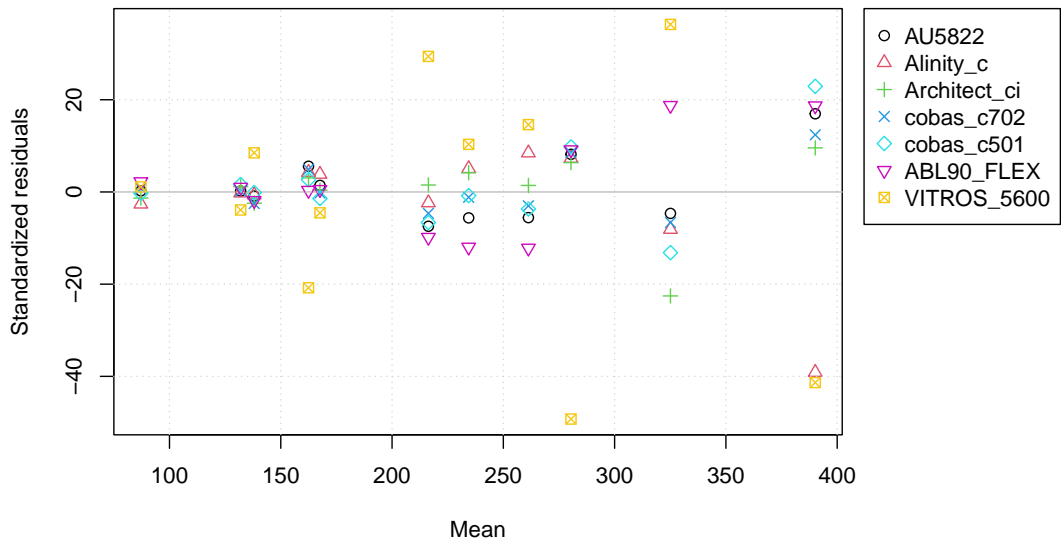


Figure 7 Residuals after scaling vs. mean for the 11 bilirubin plasma samples with 7 different assays.

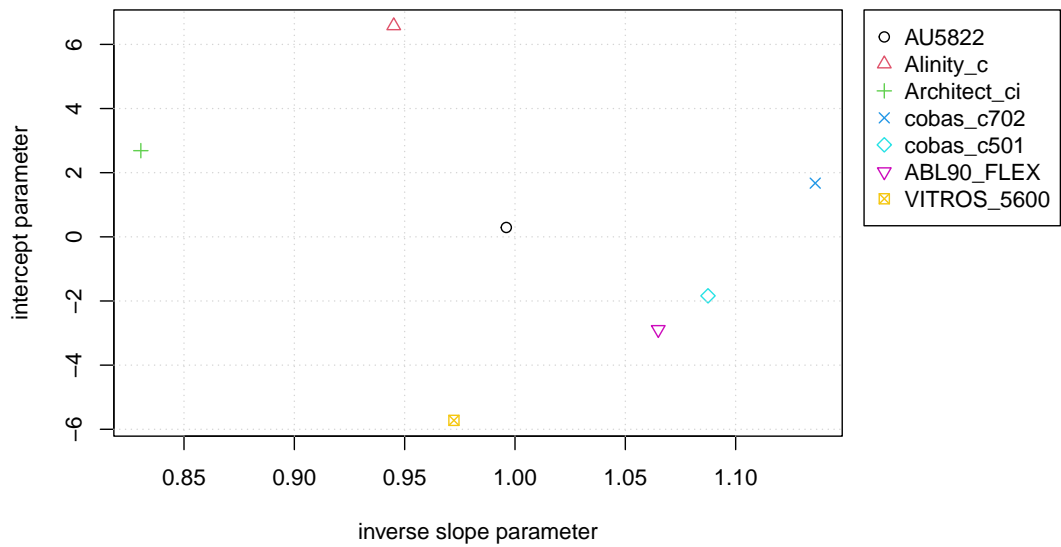


Figure 8 Intercept and inverse slope parameters of the 11 bilirubin plasma samples with 7 different assays.

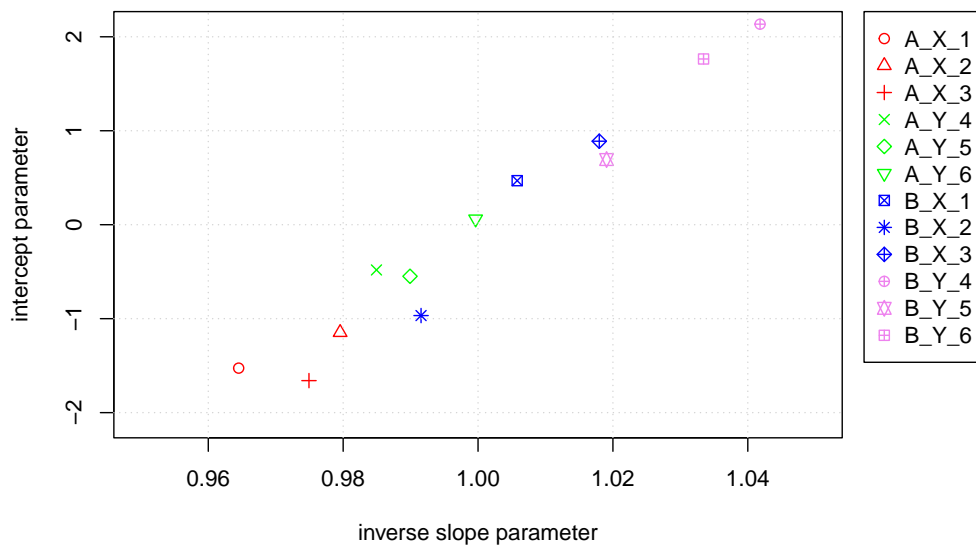


Figure 9 Intercept and inverse slope parameters for the clinical assays differing in sample preparation (A vs. B), instrument platform (X vs. Y), and reagent lot (1 to 6). Systematic differences between both instrument platform and sample preparation are clearly visible.